Low intensity conduction states in FeS_2: implications for absorption, open-circuit voltage and surface recombination

2013 J. Phys.: Condens. Matter 25 465801

(http://iopscience.iop.org/0953-8984/25/46/465801)

OPEN ACCESS

Made open access 25 November 2013

IOP PUBLISHING

JOURNAL OF PHYSICS: CONDENSED MATTER

J. Phys.: Condens. Matter **25** (2013) 465801 (10pp)

doi:10.1088/0953-8984/25/46/465801

Low intensity conduction states in FeS_2: implications for absorption, open-circuit voltage and surface recombination

P Lazić[1], R Armiento[2], F W Herbert[1], R Chakraborty[3], R Sun[1], M K Y Chan[4], K Hartman[1], T Buonassisi[3], B Yildiz[5] and G Ceder[1]

[1] Department of Materials Science and Engineering, Massachusetts Institute of Technology, Cambridge, MA 02139, USA
[2] Department of Physics, Chemistry and Biology (IFM), Linköping University, SE-58183 Linköping, Sweden
[3] Department of Mechanical Engineering, Massachusetts Institute of Technology, Cambridge, MA 02139, USA
[4] Centre for Nanoscale Materials, Argonne National Laboratory, Argonne, IL 60439, USA
[5] Department of Nuclear Science and Engineering, Massachusetts Institute of Technology, Cambridge, MA 02139, USA

E-mail: gceder@mit.edu

Received 16 April 2013, in final form 24 September 2013
Published 21 October 2013
Online at stacks.iop.org/JPhysCM/25/465801

Abstract

Pyrite (FeS_2), being a promising material for future solar technologies, has so far exhibited in experiments an open-circuit voltage (OCV) of around 0.2 V, which is much lower than the frequently quoted 'accepted' value for the fundamental bandgap of ∼0.95 eV. Absorption experiments show large subgap absorption, commonly attributed to defects or structural disorder. However, computations using density functional theory with a semi-local functional predict that the bottom of the conduction band consists of a very low intensity sulfur p-band that may be easily overlooked in experiments because of the high intensity onset that appears 0.5 eV higher in energy. The intensity of absorption into the sulfur p-band is found to be of the same magnitude as contributions from defects and disorder. Our findings suggest the need to re-examine the value of the fundamental bandgap of pyrite presently in use in the literature. If the contribution from the p-band has so far been overlooked, the substantially lowered bandgap would partly explain the discrepancy with the OCV. Furthermore, we show that more states appear on the surface within the low energy sulfur p-band, which suggests a mechanism of thermalization into those states that would further prevent extracting electrons at higher energy levels through the surface. Finally, we speculate on whether misidentified states at the conduction band onset may be present in other materials.

(Some figures may appear in colour only in the online journal)

1. Introduction

Pyrite (FeS_2) has several appealing properties for photovoltaic applications. The absorption coefficient is large [1], of the order of 10^5 cm^{-1} at photon energies of 1.0–1.5 eV. Pyrite is abundant in nature [2], non-toxic, and, as will be further discussed in the following, is frequently quoted in the present literature to have a bandgap value of ∼0.95 eV (see, e.g., [3–9]). A fundamental bandgap of this value is close to the optimum for solar cell applications. However, experiments on pyrite for solar applications carried out in the 1980s reported an open-circuit voltage (OCV) of only about 200 mV [1]. Such a low OCV is not sufficient to achieve adequate conversion efficiencies for solar applications.

There has recently been renewed interest in understanding the reasons behind the low OCV of pyrite [10]. Suggestions include various defects [3–5, 11] (e.g., sulfur vacancies in the bulk or on the surface, or line defects); pinning of the Fermi level by surface states or grain boundaries [1, 4, 6–8]; and the possible presence of impurity phases [9, 12] (primarily marcasite). Two recent studies involving authors of the present paper have used computations to show many of these suggestions to be unconvincing [13, 14]. We also note that the current observed in photoelectrochemical cell experiments is close to the theoretical maximum for the given light intensity, further suggesting that the OCV is not lowered by trapping or recombination [1]. Hence, so far, there is no conclusive explanation as to why the OCV of pyrite is so much lower than 0.95 eV.

1.1. Rethinking the pyrite bandgap

The primary sources for the often quoted 'accepted' value of the pyrite bandgap in the present literature appear to be a set of absorption experiments interpreted to show an optical bandgap value of ∼0.95 eV [15–23]. Despite these experiments formally being of the optical bandgap, past works discussing the low OCV of pyrite typically compare this value directly with quasiparticle bandgaps from computational methods [3–9]. In general, these two gaps can differ substantially, with the OCV being limited by the fundamental bandgap. The optical gap may be larger than the fundamental gap if the transition associated with the fundamental gap is indirect or dipole forbidden. There are also mechanisms that can allow absorption at energies below the fundamental gap, e.g., excitons (these and other mechanisms are discussed in more detail below). While this issue is sparsely discussed in past works, the possible discrepancy between the two gaps may have been disregarded based on that (i) the gap transition in pyrite is not dipole forbidden; (ii) pyrite band structure suggests a negligible difference between the smallest direct gap and indirect gap; and (iii) there is no *a priori* reason to expect unusually large excitonic effects in pyrite, which thus would be expected to be on the order of 10–100 meV given the dielectric constant of pyrite [24]. However, when we further investigate the published absorption experiments, there appears to be some room for interpretation of the energy where the absorption edge starts. Indeed, an early work of Ferrer *et al* [19] comments on the general discrepancy of prior results and remarks among the conclusions that the flat nature of the band edge in pyrite prevents accurate determination of the bandgap using methods that assume a parabolic band behavior.

We also find results of purely computational methods on the pyrite electronic structure to be in major disagreement on the magnitude of the quasiparticle (fundamental) bandgap, calculated as the difference between the highest occupied and lowest unoccupied states. This gap is also known as the HOMO–LUMO gap. Several works in the past have used density functional theory (DFT) [25, 26] with semi-local functionals and the $+U$ framework [27–30] to find quasiparticle bandgaps of ≈1 eV [13, 14, 31]. However, recent computations with GW find a HOMO–LUMO gap of 0.4 eV, whereas the same authors find a HSE06 hybrid functional [32, 33] gap of 2.70 eV [13, 31]. This is unusual for 'beyond semi-local DFT' methods, where successfully applied GW, hybrid functionals and DFT + U tend to roughly agree on an expanded gap compared to that of DFT with LDA or GGA functionals.

In the light of these findings, the present paper puts forward a set of arguments in support of re-examining the bandgap value of 0.95 eV presently quoted in the literature for comparison with quasiparticle bandgaps and the OCV. Specifically, our focus is on the difference between pyrite and typical semiconductor systems in that the origin of the bottom of the pyrite conduction band is a low intensity band originating from the sulfur p states. However, around 0.5 eV further into the conduction band, the contributions from other quasiparticle bands give a sharp rise in the number of conduction band states with more typical parabolic behavior. The optical spectrum from the sulfur p-band in pure bulk pyrite is of a magnitude and shape where it would overlap with the contribution from defects and disorder and thus easily be discounted in a determination of the optical band gap.

We emphasize that the present investigation is not in itself sufficient proof that the fundamental bandgap of pyrite is significantly smaller than 0.95 eV. However, the consequence of an unusual shape of the conduction band onset is rarely discussed in prior works. The main contribution of the present paper is to show that an interpretation of absorption into a low intensity sulfur p-band is in principle compatible with currently available experimental data. Pyrite makes a particularly interesting case for this discussion, since this gives a possible alternative explanation of the low OCV observed experimentally.

1.2. Optical absorption

The most commonly discussed sources of optical absorption of photons of energy smaller than the fundamental bandgap are (i) random defects, whose high concentrations may give rise to large bandwidth defect states that merge with the conduction band to give a tail-like shape at the bottom of the band [34], and (ii) a disordered structure giving an Urbach tail in the absorption spectrum [35]. Generally less discussed, but possible, are (iii) intraband excitations, where p-type defects open up states at the top of the valence band that can accept a continuum of excitations from lower energy states in the valence band, and a similar effect for n-type defects, where electrons at the edge of the conduction band can be excited to higher states; (iv) excitons can reduce the optical bandgap. However, we suggest that, aside from all these alternatives, one also needs to consider the possibility that the beginning of the conduction band in the pure bulk material may allow only very few states. In pyrite the relatively low density of lower energy conduction band states would produce optical absorption at levels indistinguishable from the other three contributions listed above. By contrast, the sudden onset of absorption for photons of energies above 0.95 eV is consistent with the appearance of a high density of states for such

energies. To make our discussion clear, we shall in the following distinguish between the 'tail states', which pertain to defects and disorder, and the '*trailing*' conduction band states that represents the true bottom of the conduction band, even in the bulk. This distinction is important, because the tail states caused by extrinsic defects or a disordered structure can, presumably, be suppressed by high-purity fabrication techniques, as is common in the silicon industry.

A material with significant intraband absorption would have a reduced efficiency, but since the intraband absorption does not affect excitations across the gap, it should thus not affect the OCV. However, if a fraction of the absorption below the apparent main absorption edge goes to the bulk conduction band, these states limit the OCV regardless of the sample purity, giving at the same time a contribution to absorption comparable to defect related tails.

Excitons usually introduce sharp peaks at the absorption edge that potentially may lower the absorption onset from the fundamental bandgap by the value of the exciton binding energy. Recent works find that the typical exciton binding energy in semiconductors is of the order of 10–100 meV, and is inversely related to the dielectric constant [24, 36]. The dielectric constant of pyrite is rather large (∼26) [37], mostly because of the large polarizability of the S^{-2} ions. Hence, the local Coulomb interactions are very much screened and excitonic effects are not expected to be large, which suggests that this is not a major contribution to the possible discrepancy between different bandgaps. Nevertheless, future work could find pyrite to exhibit highly unusual exciton properties, and if so, this is indeed a possible alternative explanation for the low OCV that we do not further investigate in the present work.

2. Computational methods

For the computational part of this study we use Kohn–Sham (KS) DFT [25, 26] with projector augmented waves (PAW) pseudopotentials [38, 39] and the PBE functional [40], as implemented in the VASP 5.1 software package [41, 42]. Our bulk calculations are performed with a cutoff of 400 eV and a converged k-point density of 24 × 24 × 24 in a Monkhorst–Pack grid [43], and 250 extra empty bands to converge the optical tensor. Our slab calculation consists of eight layers of pyrite, 10 Å of vacuum, and is sampled with an 8 × 8 × 1 k-point grid. The slab calculation uses the dipole correction implemented in VASP [44, 45]. To calculate absorption spectra we use the method described in [46]. To minimize numerical errors at small values of the absorption coefficient, care has been taken to converge the calculations in the integration denominator shift and density of states (DOS) integration step (see [46] for details). For some calculations we compare with DFT results where a $+U$ [27–30] correction is used alongside the PBE functional, which we shall refer to as PBE + U in the following. Unless specified otherwise, our computations are done with fully relaxed pyrite structures (i.e., volume, symmetry-preserving cell shape and ionic positions) starting from an experimental structure with lattice constant 5.417 Å [47]. The relaxations are done separately for PBE and PBE + U giving relaxed

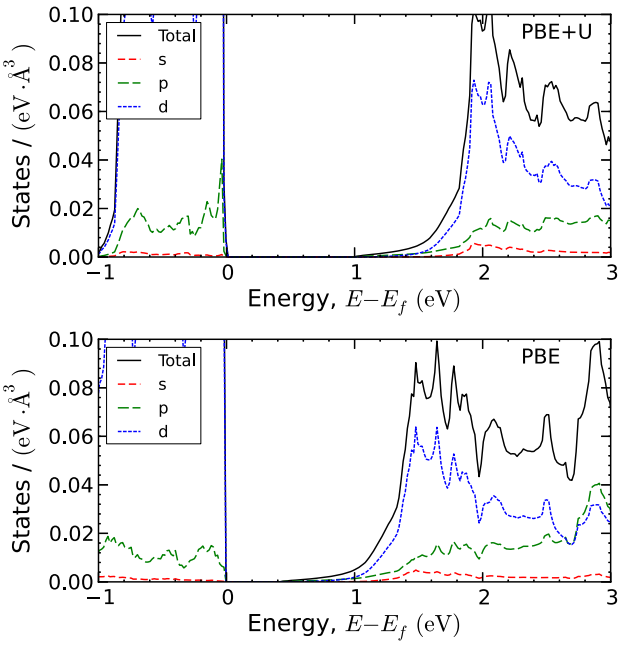

Figure 1. Density of KS states for pyrite from PBE + U (upper), and regular PBE (lower) for relaxed structures. The vertical axis is chosen to show the shape of the low density states that goes down from the conduction band in both calculations. The dashed, dash-dotted, and dotted lines are the s-, p-, and d-orbital-projected DOS, respectively.

(zero-temperature) lattice constants of 5.402 Å for PBE and 5.424 Å for PBE + U. In those calculations we use a $U - J$ value of 1.9 eV. This value is taken to represent a generally accepted value for Fe in sulfides, as was used in our previously described high-throughput framework [48], where it was obtained by a fit to experimental binary formation enthalpies [49]. It has not been fitted to a specific bandgap value.

2.1. Electronic structure

Figures 1 and 3 show the band structure of pure bulk pyrite computed with PBE and PBE + U. The axes in the DOS in figure 1 have been chosen to clearly show the shape of the bottom of the conduction band, whereas for comparison the same DOS is shown in figure 2 on axes chosen to show all DOS peaks. The DOS is also shown alongside the band structure in figure 3. As discussed above, the DFT quasiparticle (fundamental) bandgap has commonly been compared with measurements of the optical bandgap, reported as 0.95 eV [15–23]. For a relaxed pyrite crystal structure, the HOMO–LUMO bandgap gives 0.99 eV for PBE + U, and 0.42 eV without the U term. The same calculation for unrelaxed structures at the experimental ionic positions and lattice parameters gives the value 0.29 eV for PBE + U, and no gap without the U term. Regarding the description of electronic structure by PBE and PBE + U, it is not clear, in general, whether the results from relaxed or unrelaxed structures should be expected to be more accurate. However, it is common practice to consider the absolute

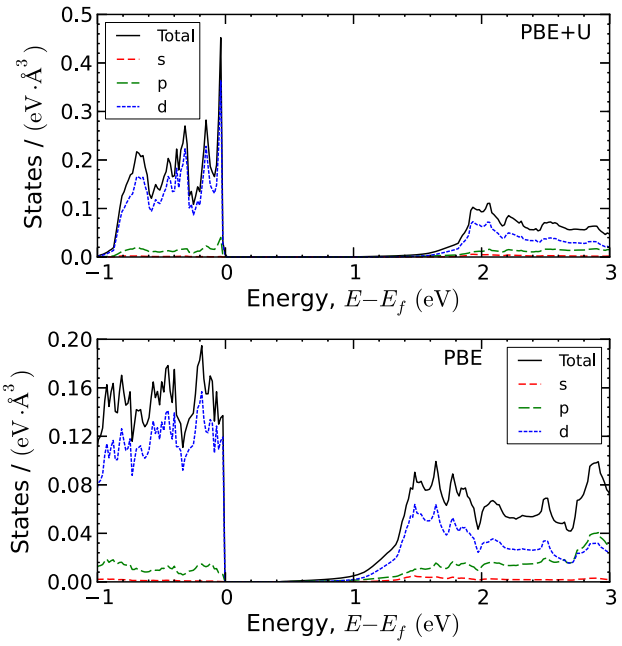

Figure 2. This figure is identical to figure 1, except that both panels are shown unzoomed, i.e., on individual *y*-scales chosen to fit all DOS peaks in the figure. This makes the nature of the low intensity states at the bottom of the conduction band more difficult to distinguish. In a less resolved DOS they may not be distinguishable at all.

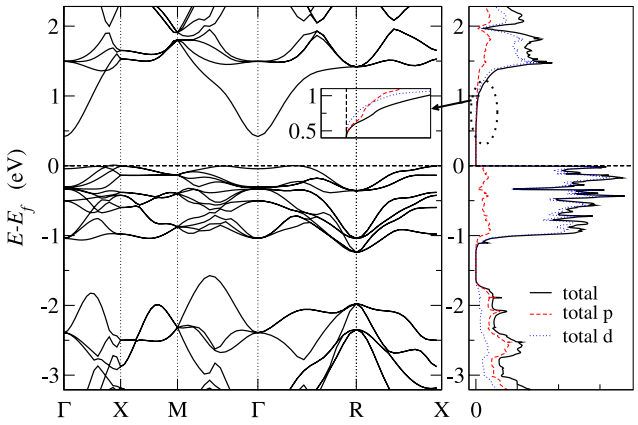

Figure 3. Band structure of bulk pyrite from PBE (left) and the corresponding DOS (right). The single p-band from sulfur dips down at the gamma point.

position of the conduction states as inaccurate in all these methods (see, e.g., [50]). For DOS and band structure, aside from an absolute shift of the conduction band, the various methods give similar results. This corroborates the common practice to take the band structure from DFT using semi-local functionals at least as a qualitative approximation of the actual band behavior. We further note that the computed bulk DOS and frequency-dependent absorption was not significantly changed when using unrelaxed crystal structures.

In the computed band structure (figure 3) we see a sulfur p-band going up from the bottom of the conduction band starting at around 0.4 eV above the Fermi level. At 0.5 eV above the bottom of this band (i.e., 0.9 eV above

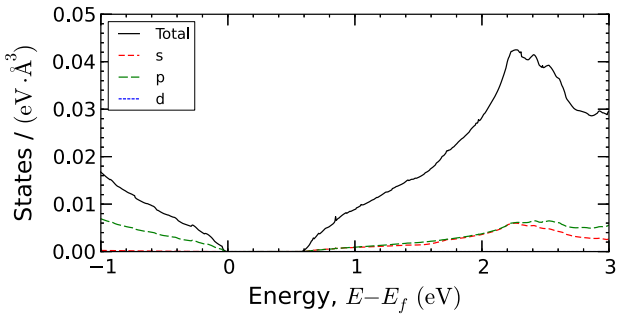

Figure 4. A closely zoomed DOS of pure bulk Si as calculated with PBE, included for comparison with figure 1. For Si the onset of the DOS is more defined, with a typical free-electron-like band shape.

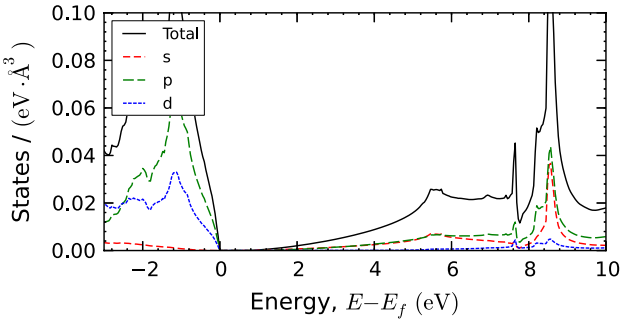

Figure 5. A closely zoomed DOS of ZnO as calculated with PBE, included for comparison with figures 1 and 4. ZnO has a DOS shape of the bottom of the conduction band that resembles that of pyrite, but lacks the sharp onset of states at a higher energy within the conduction band.

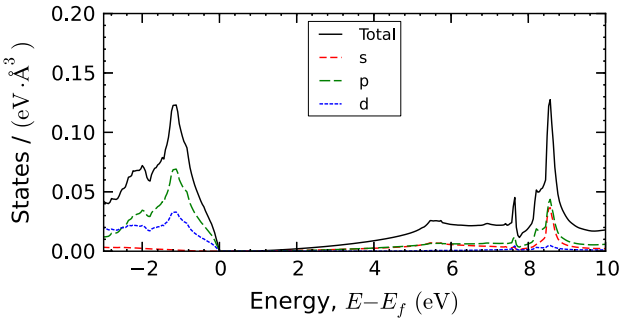

Figure 6. Identical to figure 5, except shown unzoomed for comparison with the corresponding figures for pyrite shown in figure 2. In contrast to the case of pyrite, the onset of states at the bottom of the conduction band of ZnO is equally noticeable in this figure and in figure 5.

the Fermi level) it joins other electronic bands, mostly of Fe d-symmetry. In the DOS this sulfur p-band is visible as a long narrow set of trailing states with no clear onset, reflecting the p-band parabolic dispersion in the band structure.

Pyrite differs from a prototypical semiconductor where the onset is clearer, see the DOS of silicon in figure 4. We also compare the pyrite DOS with that of bulk ZnO, as shown in figure 5 set on the same axis as figure 1. For further comparison, a version of the figure on usual axes is also shown in figure 6. The experimental ZnO fundamental bandgap is 3.3 eV which is much larger than the HOMO–LUMO gap

given from DFT with the PBE functional, 0.8 eV. Both ZnO and pyrite have a somewhat similar set of low amplitude trailing states at the bottom of the conduction band. However, the deceptive feature of pyrite is the change in nature between the low energy sulfur p-band and the sharp increase from other electronic bands ∼0.5 eV above the true bottom of the conduction band. This feature is completely missing in the case of ZnO. Hence, in a measurement that depends on the shape of the DOS at the bottom of the conduction band, such as optical absorption, it appears it should be substantially easier to identify the true bottom of the conduction band in ZnO than in pyrite. The influence on absorption experiments of this difference will be further investigated in the following.

The pyrite band structure has been found to be very dependent on the lattice parameters and the internal degrees of freedom in the structure. In [51, 52] the electronic structure of pyrite was calculated with the LDA. In [51] the authors discuss the experimentally established blueshift of the optical gap of pyrite and conclude the quasiparticle (fundamental) bandgap value to be very sensitive to the sulfur position in the unit cell. This effect appears because of the steep sulfur p-band near the Γ point at the conduction band minimum (CBM), which gives the trailing states in the DOS. Using the experimental lattice parameters the authors obtain the bandgap value of 0.85 eV, while after full relaxation they obtain a metallic structure. In contrast, [52] also finds the S-S bond distance to be the key parameter for the position of the S p states that determines the CBM and thus determines the bandgap, but obtain a bandgap value of around 1 eV for the fully relaxed structure with LDA. While some of these and our results may appear contradictory, our conclusion is that the steep sulfur p-band is a major source of difficulty also for purely theoretical methods, making the precise HOMO–LUMO difference very dependent on the details of the computation; i.e., lattice parameters, internal degrees of freedom, and exchange–correlation functional.

2.2. Absorption coefficient

We have calculated the frequency-dependent absorption coefficient using PBE and PBE + U using the method described in [46] and implemented in VASP. In this method the imaginary part of the matrix element $\varepsilon_{\alpha,\beta}(\omega)$ of the dielectric matrix for frequency ω is computed as follows:

$$\mathrm{Im}\ \varepsilon_{\alpha,\beta}(\omega) = \frac{4\pi^2 e^2}{\Omega} \lim_{q\to 0} \frac{1}{q^2} \sum_{c,v,\mathbf{k}} 2w_{\mathbf{k}} \delta(\epsilon_{c\mathbf{k}} - \epsilon_{v\mathbf{k}} - \omega) \times \langle u_{c\mathbf{k}+\mathbf{e}_\alpha q} | u_{v\mathbf{k}} \rangle \langle u_{c\mathbf{k}+\mathbf{e}_\beta q} | u_{v\mathbf{k}} \rangle^*, \quad (1)$$

where e is the electronic charge, Ω is volume of the primitive cell, $\mathbf{k}$ denotes the k-points, the indices c, v refer to the conduction and valence band states respectively, summing over all transitions from occupied to unoccupied states within the first Brillouin zone, with $\epsilon_{c\mathbf{k}}$ the corresponding eigenvalues, the vectors $\mathbf{e}_\alpha$ unit vectors for the three Cartesian directions, $w_{\mathbf{k}}$ the weight of the k-point, and $u_{c\mathbf{k}}$ the cell periodic part of the orbitals (see [46]). The real part of $\varepsilon_{\alpha,\beta}$ is then given by the Kramers–Kronig transformation

$$\mathrm{Re}\ \varepsilon_{\alpha,\beta}(\omega) = 1 + \frac{2}{\pi} P \int_0^\infty \frac{\mathrm{Im}\varepsilon_{\alpha,\beta}(\omega')\omega'}{\omega'^2 - \omega^2} \mathrm{d}\omega', \quad (2)$$

where P designates the Cauchy principal value of the integral, which is calculated numerically by the use of a small complex shift in the denominator of the integrand. The absorption coefficient $A_{\alpha,\alpha}$ can then be calculated as

$$A_{\alpha,\alpha}(\omega) = \frac{2\omega}{c} \sqrt{\frac{|\varepsilon_{\alpha,\alpha}(\omega)| - \mathrm{Re}\ \varepsilon_{\alpha,\alpha}(\omega)}{2}}, \quad (3)$$

where c is the speed of light in vacuum.

In figure 7 the result is compared with the experimental optical absorption data from various sources that, as discussed above, frequently serve as a basis for taking ∼0.95 eV as a value for the bandgap of pyrite used for comparison with quasiparticle results and the OCV. The experimental data show significant scatter, clearly illustrating the difficulty in establishing a consistent behavior of the subgap absorption. The largest differences can be explained mainly by grouping the data as either obtained from thin film or bulk samples,

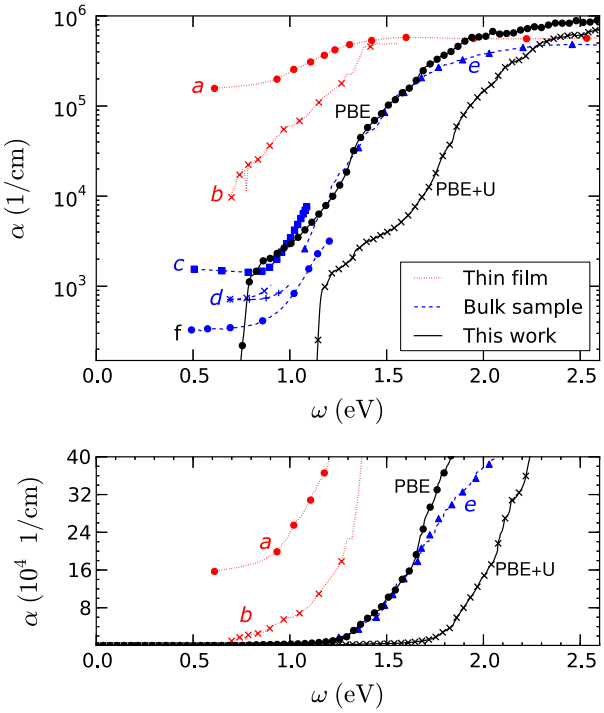

Figure 7. The onset of the frequency-dependent absorption coefficient in pyrite. Experiments for thin film and bulk samples (as labeled in the legend) are compared with our computational data. The two short curves meeting at the d label are measurements taken at 297 K (upper) and 77 K (lower). The lower graph shows the onset absorption on a linear scale as is more common. The computational results show (looking from $\omega = 0$ towards higher values, i.e. from left to right on the x-axis) first a steep incline just above the HOMO–LUMO bandgap, but only up to a relatively small absorption $\sim 10^3$ cm^{-1}, and then, as absorption happens into the trailing states at the bottom of the conduction band, a slow incline that roughly matches the subgap absorption found in absorption experiments. References for experimental data: (a) [15], (b) [16], (c) [17], (d) [18], (e) [19], (f) [20].

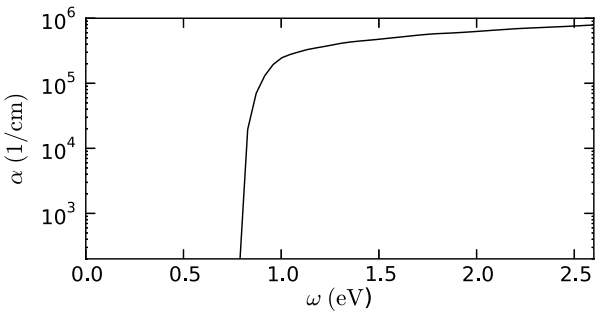

Figure 8. The onset of the frequency-dependent absorption coefficient in ZnO calculated with PBE the same way as for pyrite in figure 7. The absorption curve for ZnO shows a much more straightforward behavior, with a steep incline in absorption at the HOMO–LUMO bandgap (0.8 eV in this calculation) up to levels that should be distinguishable from contributions from defects and disorder, i.e., $>10^5$ (cm^{-1}). In contrast to the pyrite case, it appears straightforward to extract a bandgap value with good accuracy from a curve with this shape.

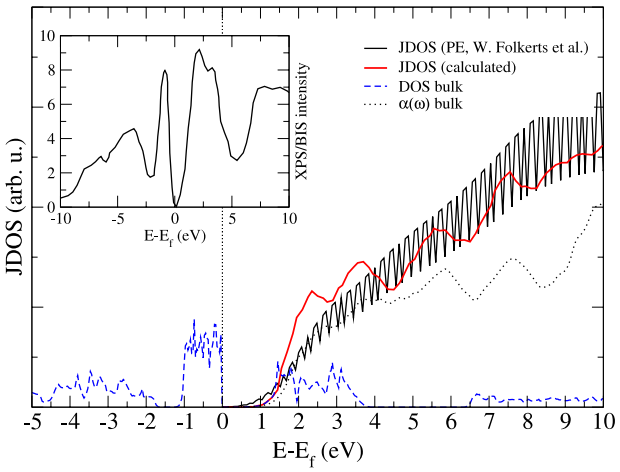

Figure 9. A comparison of the DOS and JDOS from our PBE computational results, our computed absorption, and the JDOS from the experimental photoemission data extracted from [37] (the extracted data is shown in the inset). The resolution of the experimental photoemission data is not sufficient to extract a reliable value for the fundamental bandgap, but it is clear from the figures that these data do not contradict the suggestion of a fundamental bandgap lower than 0.95 eV. Calculated optical absorption curve for bulk is also shown.

as labeled in the figure. However, all the experimental data show a significant degree of subgap absorption below 0.95 eV. In each of the cited works the absorption tails have been disregarded (usually interpreted as Urbach tails [35]) when determining the optical gap. The very steep slope at the lowest energies of the PBE and PBE+U absorption graphs in figure 7 close to (but not exactly at) the computational bandgaps are technically the true absorption edges. These appear in this figure at slightly higher energies than the HOMO–LUMO bandgap values (0.42 and 0.99 eV for PBE and PBE + U, respectively) due to the cut used for the logarithmic scale in the figure, and because the complex shift used in the integrand of equation (2) slightly affects the values when the absorption value is very low.

We suggest not to compare the absolute values of the computational results and experiments too closely. Our main conclusion from figure 7 is rather that the computational data qualitatively show an absorption tail with a strong exponential onset only about 0.5 eV *above* the true bottom of the conduction band. The computational data appear similar in general shape to subgap absorption found in the experiments. However, for the computational results we know that the absorption tails cannot be due to defects or disorder, since the computations are performed on a perfectly pure pyrite crystal, and thus are caused by the absorption into the low energy sulfur p-state in the bulk. This result should be compared with the common practice in interpretation of experiments to attribute essentially all exponential absorption tails to crystalline bulk imperfection from defects, a disordered structure, or other side effects such as holes in the sample or light scattering (see [15–23]).

The behavior of the pyrite absorption is qualitatively different from the clearer absorption edge onset observed and calculated for other semiconductors. While ZnO also has an extended increase of states in the DOS that start at the conduction band minimum, there is just one single clear absorption onset precisely at the bottom of the conduction band (0.8 eV above the valence band maximum). This is seen in figure 8, which shows the absorption coefficient of ZnO calculated in the same way as for pyrite.

At this point, it is relevant to ask whether the low intensity onset of the optical absorption curve is predominately caused by small matrix elements for the relevant transition across the bandgap, or simply because of the low intensity DOS at the bottom of the conduction band. Choi *et al* discuss in detail the various optical transitions in the pyrite band structure [31] and find that, while the transition across the fundamental gap is not dipole forbidden, the corresponding matrix element is of reduced amplitude since the conduction band minima associates rather purely with Sppσ^* orbitals and the valence band states mostly localize around the Fe atoms. In contrast, [52] suggests that the matrix elements are large because of the different orbital composition of the valence band maximum (VBM) (d) and the CBM (p). To investigate this further we compare the joint density of states (JDOS) [53][6] with the computed optical absorption, shown in figure 9. The JDOS gives an estimate of the absorption that disregards the magnitude of the matrix element. The result is that the weak onset of the optical absorption can indeed entirely be accounted for by the weak trailing states in the DOS.

The quasiparticle (fundamental) HOMO–LUMO bandgap from usual semi-local functionals such as PBE is known to usually give significantly smaller bandgaps for semiconductors than the experimental values (though, this is not *universally* true; see, e.g., figure 1 in [50] and the results for bulk PbS in [54]). However, for FeS_2, one can speculate that the large sensitivity of the bandgap to the internal degrees of freedom makes it *possible* that the error of the PBE relaxed

[6] JDOS$(E) \propto ((\rho_c(E_1))^{-1} + (\rho_v(E_2)^{-1}))^{-1}$, $E = |E_1 - E_2|$, ρ—density of states, for c-conduction, and v-valence states.

cell is such that the PBE bandgap is unusually close to the true fundamental bandgap. Nevertheless, even under the assumption that the fundamental bandgap is larger than found at this level of theory, i.e., 0.4 eV (or 0 if using the unrelaxed structure) there is some room up to the value of 0.95 eV. The PBE + U HOMO–LUMO gap is 1.0 eV, but changes with the choice of the value of U, which, in theory, allows for the possibility that a computation on a fully relaxed structure with a U parameter of the magnitude similar to that used in prior works may have given a DFT+U quasiparticle bandgap that is larger than the true fundamental bandgap. We do not think this is an unreasonable suggestion, given the major disagreement between PBE + U and other higher level theories, i.e., GW (0.4 eV) and hybrid functionals (2.7 eV). The lower graph of figure 7 indeed suggests that the PBE + U HOMO–LUMO gap may be too large since it reproduces the main onset of absorption at a significantly higher energy than found experimentally, although this conclusion may be affected by various causes of absorption below the fundamental gap discussed above, e.g., excitons. However, as also explained above, it appears unlikely for excitons to account for the full discrepancy at absorption edge onset. Such a conclusion is in further disagreement with the observation by other authors that optical features associated with the intraband critical points are well reproduced with PBE and GW, but the +U correction places them at energies too high by 0.3–0.5 eV [31].

2.3. Comparison with other experiments

Our focus has so far been to investigate the absorption data to which we have traced the 0.95 eV value used in the present literature. However, one may argue that there are experiments more suited for extracting a value for the fundamental bandgap. One such experiment would be photoemission. However, we are only aware of a single such experimental work on pyrite by Folkerts *et al* [37]. These authors do not extract a value of the fundamental bandgap from their data independently from the prior absorption experiments. In figure 9 we compare our computational data with their experiment. While the photoemission data appear to indicate states far below 0.95 eV, the resolution of this experiment is simply too low to resolve a difference in bandgap needed for the present investigation. We also note that the photoemission experiments may be influenced by the electronic structure on the pyrite surface, further complicating the analysis of these data. Nevertheless, to the extent that a conclusion can be drawn, these data are not in contradiction with a fundamental bandgap below 0.95 eV.

Other available experiments from which the pyrite bandgap can be extracted include the use of the exponential relations between either the resistivity, conductivity, or the Hall coefficient and inverse temperature [55, 22, 56]. A bandgap value is then usually extracted from the slope of, e.g., the resistivity in the high temperature limit of a logarithmic plot. These experiments, as any other experimental technique that depends on the shape of the density of states of the conduction band, will be subject to a possibly similar misidentification of the trailing bulk states as discussed in this paper for absorption. The contribution from the trailing states will mix with that of defects and disorder and appear exceedingly small next to the more apparent onset at higher energy. The situation where trailing states have a major influence is in determining the quantities that depend on the very absolute CBM position in a very pure sample, e.g., the measurement of the OCV in a typical setup. In contrast, for the specific case of resistivity versus inverse temperature, the slope in the high temperature limit would arguably be determined by the more apparent conduction band onset, whereas the true fundamental bandgap, which takes into account the trailing states from the sulfur p-band, would have to be determined from a region of linear slope at intermediate temperatures that may be easy to overlook.

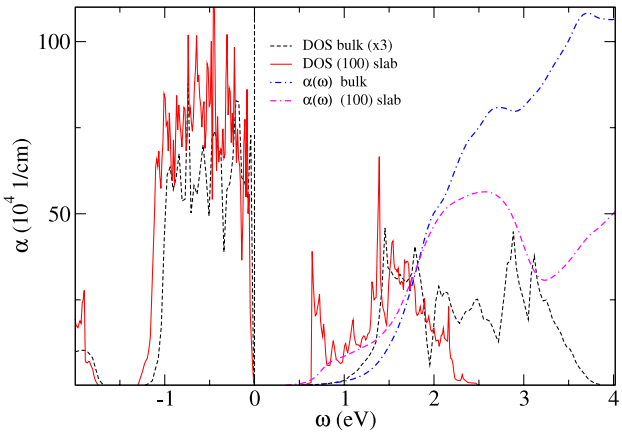

Figure 10. The calculated frequency-dependent optical absorption coefficient for bulk pyrite and a (100) surface slab (eight layers thick). Note that slab and bulk quantities are aligned with the top of the respective valence bands, which may be at different absolute energies. The calculated bulk DOS is also plotted for comparison.

2.4. Surface effects

Separate from our suggestion that low amplitude trailing states are present at the bottom of the conduction band in bulk pyrite, we now turn to the possible additional influence of surfaces on the electronic states of pyrite. In figure 10 we superimpose the computed (100) surface DOS and absorption coefficient on the corresponding bulk quantities. Surface states typically appear in the fundamental bandgap of the bulk [57]. However, in the case of pyrite, surface states appear continuously connected to the conduction band. The (111) surface behaves similarly (not shown). These results can be compared to the normalized conductance from experimental scanning tunneling spectroscopy (STS) data. This picture is supported by experimental evidence from STS, shown in figure 11. The measurements were done on a synthetic pyrite sample produced by similar methods as those described in [58]. Our STS data resemble that of Rosso *et al* [59] and have been obtained using similar methods. An enlightening comparison can be made with the normalized conductance for the Si surface in [60]. The latter has a longer and more pronounced flat region than found for pyrite. It is

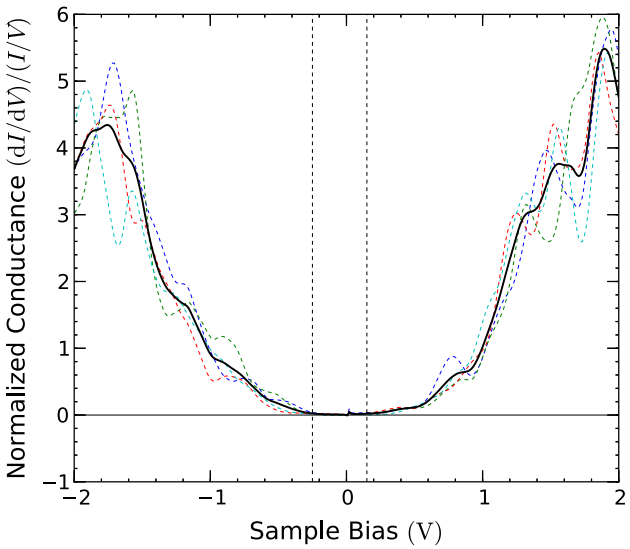

Figure 11. Normalized conductance from experimental STS data for the pyrite (100) surface for a synthetic sample. The solid line is the average of four measurements taken on the same sample (dashed lines), which are included to illustrate the overall uncertainty. The normalized conductance is expected to reproduce features of the *surface* DOS, see figure 10. All the data sets consistently suggest a fundamental bandgap for the surface of ∼0.4 eV, shown with vertical lines, which is smaller than that found with both PBE and PBE + U for a slab system. The recent extensive STS study of pyrite is given in reference [67].

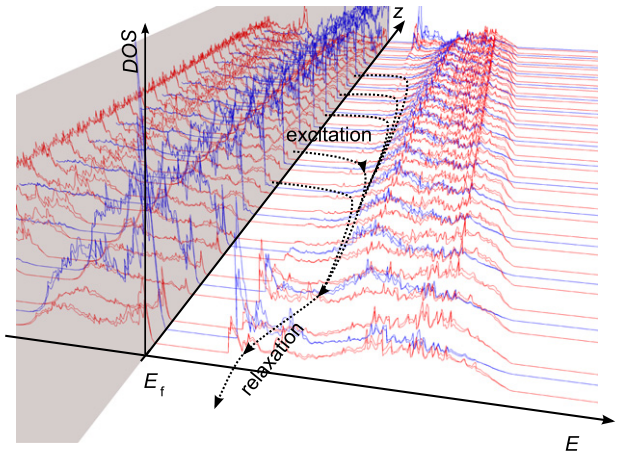

Figure 12. The atom-projected DOS per atomic layer in a very thin (around 20 Å thick) pyrite surface slab. Red lines represent sulfur atoms, and blue lines iron atoms. The gray region marks states in the valence band. The black arrows shows our suggested mechanism for rapid dissipation as electrons are extracted from the sample through a surface (located at $z = 0$).

typically difficult to quantify the fundamental bandgap of a semiconductor directly from the STS data with a high level of accuracy [61]. Nevertheless, it appears that the fundamental bandgap on the surface given by the STS data is smaller than the one we obtain with DFT using the PBE functional for the surface [62].

In addition to the discussion above suggesting the possibility that the low OCV observed for pyrite can be explained as a misinterpretation of optical data for determining the fundamental bulk bandgap of pyrite, we will discuss a surface mechanism that may be responsible for further restriction of the OCV. The mechanism applies to a situation in which electrons are excited above 1 eV, and for some reason still can be extracted through the surface of the pyrite crystal, despite the low fundamental bulk bandgap. This could be the case, for example, in high intensity light conditions applied to pyrite thin film. Such light conditions could fill up the bulk tail states (bottom of the CB) in the dynamic Burstein–Moss effect [63], and make the effective fundamental bandgap increase above the tail states. Our best estimate, without knowledge of the recombination time, indicates that this would require very high intensity or a very thin sample. From the DOS in figure 1 we can estimate the electron concentration needed to completely fill up the trailing states up to the more apparent band onset as ∼0.001 electrons $Å^{-3}$ (10^{21} electrons cm^{-3}), but given the shape of the trailing states, a partial effect may be seen at much lower intensities.

The mechanism that we propose is the following: electrons excited in the bulk that are being extracted through the surface layers would pass through few atomic layers with smooth and gapless connection to the higher-density surface states shown in figure 10 and would thermalize quickly into those surface states. We expect thermalization to be very rapid [64] because it occurs within a single band which terminates in surface states (intraband relaxation within the sulfur p-band). As such, dissipation is suggested to take place on the femtosecond scale [65]—even if excitations could occur in the bulk at a higher level, these electrons would not contribute to higher effective OCV. (See figure 12 for an illustration of how bulk excited states thermalize on their way to the surface.) One conclusion is that despite the issue of a possibly low fundamental bulk bandgap, surface passivation of pyrite thin film may still be a possible way towards an improved OCV in certain configurations. Surface passivation was explored by Antonucci *et al* who reported an improved OCV [66]. However, in this specific case the sample was so thin that the surface passivation may actually have changed the nature of the bulk crystal completely, possibly removing the intrinsic bulk tail.

3. Summary and conclusions

In conclusion, in this work we have found that a theoretical analysis of data for pure bulk pyrite supports the existence of low density trailing states at the bottom of the conduction band which are not due to defects or structural disorder. We have generally established that this behavior of the conduction band states would be observed in absorption experiments with the shape and magnitude very similar to that of defects and disorder. Combined with discrepancies in the subgap absorption in earlier experiments and an unusually high level of disagreement between ‘beyond semi-local DFT’ computational methods, we suggest that there are grounds for a future re-examination of the accepted value of the fundamental bandgap of pyrite. One can speculate whether

the same error possibly appears for any other materials with similar trailing states. For a material where the DOS does not have a clear onset, any error made will systematically be towards higher gap values. As seen in the case of pyrite, such errors could be substantial, and caution is needed when relying on the quoted bandgap values of less well-studied compounds, as is, for example, common practice when benchmarking computational methods. Our findings also constitute an important general warning about dismissing subgap absorption without taking into account the possibility of the onset DOS having an *unusual* shape.

Finally, we summarize here the arguments from both the present work and elsewhere that we have put forward for the need to re-examine the fundamental bandgap of pyrite: (i) the HOMO–LUMO bandgap calculated with higher order methods does not consistently extend the semi-local KS DFT gap in the usual way; instead, the GW as higher order method accepted as most accurate, preserves the PBE bandgap of 0.4 eV [31]; (ii) the dielectric function as calculated with semi-local KS DFT and GW, both with 0.4 eV HOMO–LUMO gap values, matches experiment in the entire energy range, rather than giving a shifted spectrum [31]; (iii) STS data suggest that PBE may not underestimate the fundamental *surface* bandgap in pyrite; (iv) available experimental data presently used to support the fundamental bulk bandgap value of 1 eV appears to also be compatible with an alternative interpretation of a smaller fundamental bandgap, but with a region of low intensity states at the bottom of the conduction band that would not be part of the primary absorption edge seen around 1 eV in absorption experiments; (v) the existence of a low intensity region with a sudden larger onset at higher energies for absorption into the conduction band is supported by DFT calculations using various approximations.

Acknowledgments

RA, PL, RS, MKYC, and GC acknowledge support from the Chesonis Family Foundation and DOE grant DE-FG02-96ER45571. RC and KH acknowledge the National Science Foundation. FWH and BY acknowledge support from BP PLC through the BP-MIT Center for Materials and Corrosion. RA acknowledge funds provided by the Swedish Research Council (VR) grant 621-2011-4249 and the Linnaeus Environment at Linköping on Nanoscale Functional Materials (LiLi-NFM) funded by VR. This work was sponsored in part by Robert Bosch LLC through Bosch Energy Research Network Grant no. 02.20.MC11. This work was performed, in part, at the Center for Nanoscale Materials, a US Department of Energy, Office of Science, Office of Basic Energy Sciences User Facility under Contract No. DE-AC02-06CH11357. We thank K J Van Vliet for helpful discussion.

References

[1] Ennaoui A, Fiechter S, Pettenkofer C, Alonso-Vante N, Büker K, Bronold M, Höpfner C and Tributsch H 1993 *Sol. Energy Mater. Sol. Cells* **29** 289
[2] Murphy R and Strongin D R 2009 *Surf. Sci. Rep.* **64** 1
[3] Birkholz M, Fiechter S, Hartmann A and Tributsch H 1991 *Phys. Rev.* B **43** 11926
[4] Bronold M, Pettenkofer C and Jaegermann W 1994 *J. Appl. Phys.* **76** 5800
[5] Abd El Halim A, Fiechter S and Tributsch H 2002 *Electrochim. Acta* **47** 2615
[6] Bronold M, Büker K, Kubala S, Pettenkofer C and Tributsch H 1993 *Phys. Status Solidi* a **135** 231
[7] Guanzhou Q, Qi X and Yuehua H 2004 *Comput. Mater. Sci.* **29** 89
[8] Cai J and Philpott M R 2004 *Comput. Mater. Sci.* **30** 358
[9] Wadia C, Wu Y, Gul S, Volkman S K, Guo J and Alivisatos A P 2009 *Chem. Mater.* **21** 2568
[10] Zhang Y N, Hu J, Law M and Wu R Q 2012 *Phys. Rev.* B **85** 085314
[11] von Oertzen G U, Skinner W M and Nesbitt H W 2005 *Phys. Rev.* B **72** 235427
[12] Spagnoli D, Refson K, Wright K and Gale J D 2010 *Phys. Rev.* B **81** 094106
[13] Sun R, Chan M K Y and Ceder G 2011 *Phys. Rev.* B **83** 235311
[14] Sun R, Chan M K Y, Kang S Y and Ceder G 2011 *Phys. Rev.* B **84** 035212
[15] Sato K 1984 *J. Phys. Soc. Japan* **53** 1617
[16] Smestad G, Ennaoui A, Fiechter S, Tributsch H, Hofmann W K, Birkholz M and Kautek W 1990 *Sol. Energy Mater.* **20** 149
[17] Schlegel A and Wachter P 1976 *J. Phys. C: Solid State Phys.* **9** 3363
[18] Kou W W and Seehra M S 1978 *Phys. Rev.* B **18** 7062
[19] Ferrer I J, Nevskaia D M, de las Heras C and Sánchez C 1990 *Solid State Commun.* **74** 913
[20] Ennaoui A, Fiechter S, Goslowsky H and Tributsch H 1985 *J. Electrochem. Soc.* **132** 1579
[21] Marinace J C 1954 *Phys. Rev.* **96** 593
[22] Bither T A, Bouchard R J, Cloud W H, Donohue P C and Siemons W J 1968 *Inorg. Chem.* **7** 2208
[23] Horita H and Suzuki T 1980 *Japan. J. Appl. Phys.* **19** 391
[24] Dvorak M, Wei S-H and Wu Z 2013 *Phys. Rev. Lett.* **110** 016402
[25] Hohenberg P and Kohn W 1964 *Phys. Rev.* **136** B864
[26] Kohn W and Sham L J 1965 *Phys. Rev.* **140** A1133
[27] Anisimov V I, Zaanen J and Andersen O K 1991 *Phys. Rev.* B **44** 943
[28] Anisimov V I, Solovyev I V, Korotin M A, Czyżyk M T and Sawatzky G A 1993 *Phys. Rev.* B **48** 16929
[29] Liechtenstein A I, Anisimov V I and Zaanen J 1995 *Phys. Rev.* B **52** R5467
[30] Dudarev S L, Botton G A, Savrasov S Y, Humphreys C J and Sutton A P 1998 *Phys. Rev.* B **57** 1505
[31] Choi S G, Hu J, Abdallah L S, Limpinsel M, Zhang Y N, Zollner S, Wu R Q and Law M 2012 *Phys. Rev.* B **86** 115207
[32] Heyd J, Scuseria G E and Ernzerhof M 2003 *J. Chem. Phys.* **118** 8207
[33] Krukau A V, Vydrov O A, Izmaylov A F and Scuseria G E 2006 *J. Chem. Phys.* **125** 224106
[34] Grundmann M 2006 *The Physics of Semiconductors: An Introduction Including Devices and Nanophysics* (Berlin: Springer)
[35] Urbach F 1953 *Phys. Rev.* **92** 1324
[36] Wannier G 1937 *Phys. Rev.* **52** 191
[37] Folkerts W, Sawatzky G A, Haas C, de Groot R A and Hillebrecht F U 1987 *J. Phys. C: Solid State Phys.* **20** 4135
[38] Blochl P E 1994 *Phys. Rev.* B **50** 17953
[39] Kresse G and Joubert D 1999 *Phys. Rev.* B **59** 1758
[40] Perdew J P, Burke K and Ernzerhof M 1996 *Phys. Rev. Lett.* **77** 3865

[41] Kresse G and Hafner J 1993 *Phys. Rev.* B **47** 558
[42] Kresse G and Furthmüller J 1996 *Phys. Rev.* B **54** 11169
[43] Monkhorst H J and Pack J D 1976 *Phys. Rev.* B **13** 5188
[44] Neugebauer J and Scheffler M 1992 *Phys. Rev.* B **46** 16067
[45] Bengtsson L 1999 *Phys. Rev.* B **59** 12301
[46] Gajdoš M, Hummer K, Kresse G, Furthmüller J and Bechstedt F 2006 *Phys. Rev.* B **73** 045112
[47] Bayliss P 1977 *Am. Mineral.* **62** 1168
[48] Jain A, Hautier G, Moore C J, Ong S P, Fischer C C, Mueller T, Persson K A and Ceder G 2011 *Comput. Mater. Sci.* **50** 2295
[49] Wang L, Maxisch T and Ceder G 2006 *Phys. Rev.* B **73** 195107
[50] Chan M K Y and Ceder G 2010 *Phys. Rev. Lett.* **105** 196403
[51] Opahle I, Koepernik K and Eschrig H 1999 *Phys. Rev.* B **60** 14035
[52] Eyert V, Höck K-H, Fiechter S and Tributsch H 1998 *Phys. Rev.* B **57** 6350
[53] See, e.g. Hamaguchi C 2010 *Basic Semiconductor Physics* 2nd edn (Berlin: Springer) chapter 4 (Section 4.3)
[54] Walsh A 2011 *Proc. R. Soc.* A **467** 1970
[55] Karguppikar A M and Vedeshwar A G 1988 *Phys. Status Solidi* a **109** 549
[56] Horita H 1973 *Japan. J. Appl. Phys.* **12** 617
[57] Zangwill A 1988 *Physics at Surfaces* (Cambridge, MA: Cambridge University Press)
[58] Lehner S W 2007 Effects from As, Co, and Ni impurities on pyrite oxidation kinetics *PhD Thesis* Vanderbilt University
[59] Rosso K M, Becker U and Hochella M F 1999 *Am. Mineral.* **84** 1535
[60] Bellec A, Riedel D, Dujardin G, Boudrioua O, Chaput L, Stauffer L and Sonnet P 2009 *Phys. Rev.* B **80** 245434
[61] Ishida N, Sueoka K and Feenstra R M 2009 *Phys. Rev.* B **80** 075320
[62] Krishnamoorthy A, Herbert F W, Yip S, Van Vliet K J and Yildiz B 2013 *J. Phys.: Condens. Matter* **25** 045004
[63] Burstein E 1954 *Phys. Rev.* **83** 632
[64] Lazić P, Silkin V M, Chulkov E V, Echenique P M and Gumhalter B 2006 *Phys. Rev. Lett.* **97** 086801
[65] Archer M D 2003 *Nanostructured and Photoelectrochemical Systems for Solar Photon Conversion* 1st edn, vol 3 (London: Imperial College Press) p 67
[66] Antonucci V, Arico' A S, Giordano N, Antonucci P L, Russo U, Cocke D L and Crea F 1991 *Sol. Cells* **31** 119
[67] Herbert F W, Krishnamoorthy A, Van Vliet K J and Yildiz B 2013 *Surf. Sci.* **618** 53